

Numerical and experimental investigation on the temperature distribution of steel tubes under solar radiation

Hongbo Liu¹, Zhihua Chen^{*1,2} and Ting Zhou¹

¹*Department of Civil Engineering, Tianjin University, Tianjin, 300072, China*

²*Tianjin Key Laboratory of Civil Engineering Structure & New Materials, Tianjin University, Tianjin, 300072, China*

(Received January 18, 2011, Revised July 25, 2012, Accepted August 7, 2012)

Abstract. The temperature on steel structures is larger than the ambient air temperature under solar radiation and the temperature distribution on the affected structure is non-uniform and complicated. The steel tube, as a main structural member, has been investigated through experiment and numerical analysis. In this study, the temperature distribution on a properly designed steel tube under solar radiation is measured. A finite element transient thermal analysis method is presented and verified by the experimental results and a series of parametric studies are carried out to investigate the influence of various geometric properties and orientation on the temperature distribution. Furthermore, a simplified approach is proposed to predict the temperature distribution of steel tube. Based on both the experimental and the numerical results, it is concluded that the solar radiation has a significant effect on the temperature distribution of steel tubes. Under the solar radiation, the temperature of steel tubes is about 20.6°C higher than the ambient air temperature. The temperature distribution of steel tubes is sensitive to the steel solar radiation absorption, steel tube diameter and orientation, but insensitive to the solar radiation reflectance and thickness of steel tube.

Keywords: temperature; solar radiation; steel tube; numerical analysis; simplified calculation method

1. Introduction

In recent years, more and more researchers (Huang 2010, Papadopoulos 2008) have a concern on the structural property of steel structures exposed to fire. But the temperature distribution and structural behaviour of steel structures under solar radiation is rarely referred. It is well known that many steel structures are exposed to solar radiation, such steel bridges, steel arches and some steel space structures roofed by glass or ETFE membrane. Due to the effect of solar radiation, the temperature of steel structure is significantly higher than the ambient air temperature and the temperature is non-uniformly distributed. Alinia (2006, 2007) carried out some works on thermal behaviors of spherical double layer space truss domes under uniform and un-uniform thermal loading. Fan (2007) studied the temperature distribution on the structure of China National Stadium

*Corresponding author, Professor, E-mail: zhchen@tju.edu.cn

under solar radiation. However, none of researchers has studied the temperature distribution of steel structures exposed to solar radiation by transient thermal analysis.

It is clear that the temperature distribution is important for the thermal responding analysis. Current available papers about temperature distribution research under solar radiation are mostly concentrated on the dams (Jin 2010), the bridges (Xu 2010, Kim 2010, Tong 2000) and the pavements (Brisn 2006). However, the numerical methods of temperature distribution analysis presented for dams, bridges and pavements are not applicable to the spatial steel structures, which comprise many steel tubes. Therefore, it is important to understand the temperature distribution of steel tubes through both experimental and numerical studies, and give some design recommendations for large span spatial steel structures taking account of its effects.

2. Objectives and scope of investigation

An extensive study was conducted on the temperature distribution of steel tubes, under solar radiation. The research objectives included:

- Investigate temperature distribution of steel tubes under solar radiation;
- Study the effect of various parameters on the temperature distribution of steel tubes under solar radiation.
- Present a simplified approach to predict the temperature distribution of steel tubes under solar radiation.

The following tasks were undertaken in order to achieve the above research objectives

Task 1 The temperatures in a steel tube exposed to solar radiation were measured. It not only provides insights into the temperature distribution, but also provides data to verify future numerical simulation method.

Task 2 A numerical simulation method was developed based on ASHRAE solar radiation model and transient finite element thermal analysis.

Task 3 Parameter studies were conducted to investigate the effects of various parameters on the temperature distribution of steel tubes under solar radiation.

Task 4 A simplified calculation method was developed based on steady-state thermal conductivity theory to predict the temperature distribution of steel tubes under solar radiation.

3. Experimental researches

3.1 Experiment design

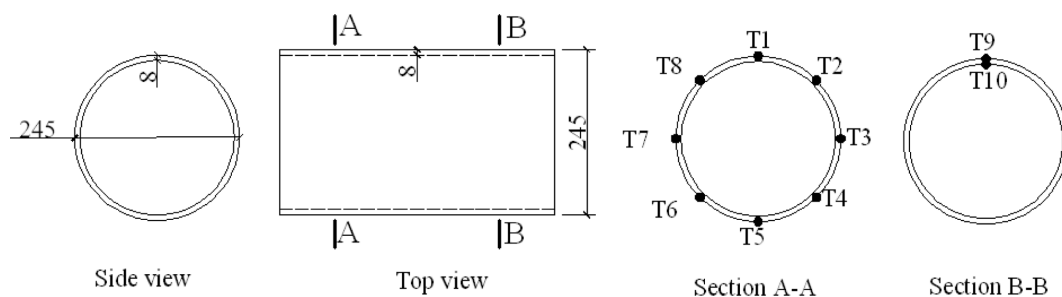
A steel tube specimen, shown in Fig. 1, is designed and tested to obtain its temperature distribution under solar radiation in summer time. In this test, infra-red temperature meter is used to collect the temperature at ten designed measure points across the tube section, shown in Fig. 2.

3.2 Results analysis

The temperatures at measure points, arranged as in Fig. 2, are recorded, respectively, at 6:00 am, 8:00 am, 10:00 am, 12:00 am, 13:00 pm, 14:00 pm, 15:00 pm, 16:00 pm, 17:00 pm, 18:00 pm and



Fig. 1 Steel tube specimen on experiment site



• Stand for the temperature measure point

Fig. 2 Arrangement of temperature measure points on the steel tube specimen

19:00 pm on 22th, 23th and 24th July, 2010.

The temperature-time curves of the maximal temperature point (Point 1) and the minimal temperature point (Point 5) for the steel tube specimen are shown in Fig. 3 and Fig. 4. The temperatures on all measure points at 14:00 pm are indicated in Fig. 5. Fig. 6 shows the temperature-time curves of Point 1, Point 9 and Point 10 . In addition, the maximal and minimal temperatures on 22th, 23th and 24th July are listed in Table 1. The above test results support following conclusions:

- 1) The temperature-time curves for Point 1 and Point 5 are approximately sine curves as shown in Fig. 3 and Fig. 4.
- 2) The maximal temperature, shown in Table 1, in this test is 54.3°C, which is 20.1°C higher than the corresponding ambient air temperature; and the maximal temperature occurs at 12:00~14:00.
- 3) The temperatures of the steel tube specimen increase initially and then decrease from Point 1 to Point 8 at 14:00 pm, and the point-temperature curve is similar to sine curve as it shown in Fig. 5.
- 4) The temperature-time curve of Point 9 is identical with that of measure Point 10, shown as Fig. 6; therefore, the temperature in thickness direction is uniform.
- 5) The temperature-time curve of measure Point 1 is identical with that of measure Point 9, shown as Fig.6; therefore, the temperature in axis direction is uniform.

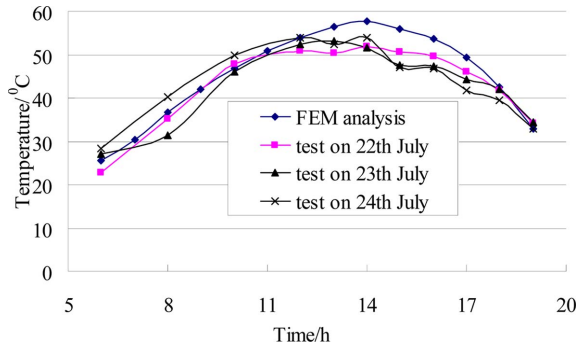


Fig. 3 Time-temperature curve of Point 1

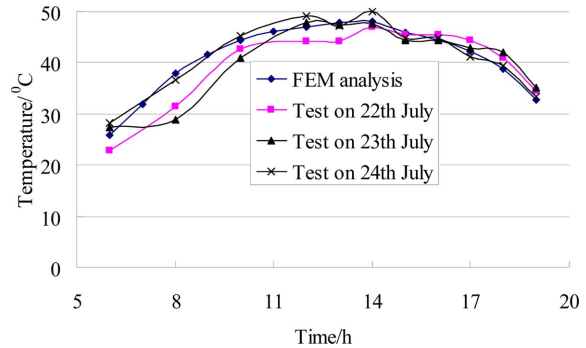


Fig. 4 Time-temperature curve of Point 5

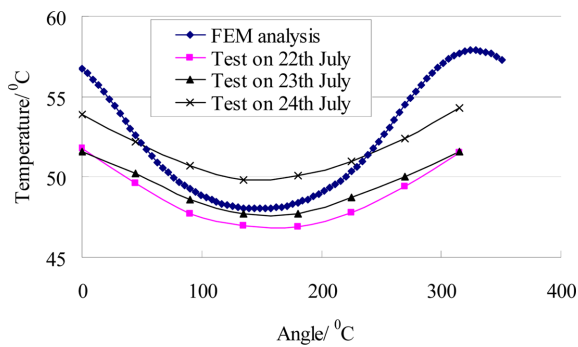


Fig. 5 Point-temperature curve at 14:00

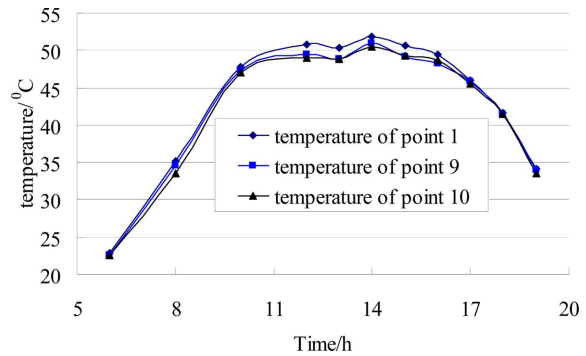


Fig. 6 Time-temperature curve of Point 1 and Point 9

Table 1 Daily minimal temperature of steel tube specimen at 14:00

	$T_{\text{test}22}$	$T_{\text{test}23}$	$T_{\text{test}24}$	T_{FEM}	Error-max
Min temperature	46.9	47.7	49.8	48.1	2.6%
Max temperature	51.8	51.6	54.2	57.9	12.2%

4. Numerical simulation

Temperature distribution within a steel tube is governed by heat conduction inside its body and the convective and radiative heat exchanging with the surrounding environment. For any steel tube exposed to solar radiation, the heat flow acting on the outer surface includes convection, solar radiation, and long wave radiation.

4.1 Solar radiation model

The ASHRAE clear-sky model was adopted in this study to calculate the solar radiation striking the surface of steel tubes (Faye 2005). In this model, the total global solar radiation is assumed to be the sum of direct radiation, diffuse radiation, and the solar radiation reflected from the

surrounding surface.

At the earth's surface on a clear day, the value of solar radiation is calculated by following equation

$$G_{ND} = \frac{A}{\exp(B/\sin\beta)} C_N \tag{1}$$

Where: G_{ND} = normal direct radiation, W/m^2 ; A = apparent solar radiation at air mass equal to zero, W/m^2 ; B = atmospheric extinction coefficient; β = solar altitude as it shown in Fig. 7; C_N = clearness number.

Based on the ASHRAE model, the total solar radiation incident on a non-vertical surface can be calculated by Eq. (2)

$$q_s = \varepsilon(G_D + G_d + G_R) = \varepsilon[\max(\cos\theta, 0) + CF_{ws} + \rho_g F_{wg}(\sin\beta + C)] \tag{2}$$

$$F_{ws} = (1 + \cos\alpha)/2 \tag{3}$$

$$F_{wg} = (1 - \cos\alpha)/2 \tag{4}$$

Where ε is the solar radiation absorptivity; θ is the angle of incidence between the sun's rays and the normal to the surface as it shown in Fig. 7; α is tilt angle as it shown in Fig. 7; C is obviously the ratio of diffuse irradiation on a surface to direct normal radiation; F_{ws} the angle factor between the surface and the sky; F_{wg} is the configuration or angle factor from surface wall to ground; ρ_g is the reflectance of ground or horizontal surface

Similarly, the total solar radiation incident on a vertical surface can be found by adding the individual components: direct component, sky diffuse and reflected component

$$q_s = \varepsilon(G_D + G_d + G_R) = \varepsilon \left[\max(\cos\theta, 0) + \frac{G_{dV}}{G_{dH}} C + \rho_g F_{wg}(\sin\beta + C) \right] G_{ND} \tag{5}$$

$$\frac{G_{dV}}{G_{dH}} = \begin{cases} 0.55 + 0.437\cos\theta + 0.313\cos^2\theta & \theta > -0.2 \\ 0.45 & \text{otherwise} \end{cases} \tag{6}$$

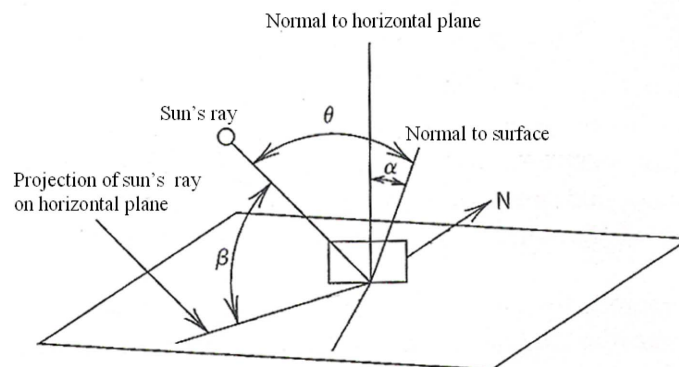


Fig. 7 Schematic diagram of angle β , θ and α

The parameters A, B, and C should be determined based on the characteristics of solar radiation at the experiment site. Unfortunately, this information is not yet available. To overcome this problem, the expressions of parameters A, B, and C for Beijing (Li 1998), near to Tianjin, are adopted to calculate solar radiation.

4.2 Long wave radiation

The long wave radiation on the surface of steel plates can be expressed by Stefan-Boltzmann equation (Faye 2005)

$$q_l = \varepsilon_f \sigma (F_{wg}(T_g^A - T^A) + F_{ws}(T_{sky}^A - T^A)) \quad (7)$$

Where ε_f is the emissivity of the radiation emitted by a steel tube surface; σ is Stefan-Boltzmann constant = 5.67×10^{-8} W/(m²·K⁴); T_{sky} is the effective temperature of sky, usually calculated by $T_a - 6$ (T_a is the corresponding ambient air temperature); T_g is the ground temperature.

In the following numerical analysis, the temperature T_a and T_g obtained in the experiment are used.

4.3 Transient thermal analysis

Transient thermal finite element analysis is conducted in this study using ANSYS software, and the main steps for this analysis are as following:

Step 1: establish the finite element model of a steel tube using SOLID70 element with small enough size (Chen 2009).

Step 2: apply the thermal load induced by solar radiation (calculated by Eq. (5) or Eq. (6)) and long wave radiation (calculated by Eq. (7)) on the outer surface of steel tube at t ; and specify the corresponding ambient air temperature for convection calculation.

Step 3: obtain the temperature distribution data from the thermal analysis results of Step 2, and calculate the thermal load at $t + \Delta t$ induced by solar radiation (calculated by Eq. (5) or Eq. (6)) and long wave radiation (calculated by Eq. (7)) on the outer surface of steel tube

Step 4: re-carry out Step 2 and Step 3 until sun set.

The physical properties of steel material adopted in the finite element model and the other main parameters referred in Eq. (1) to Eq. (7) are listed in Table 2.

Table 2 Parameters adopted in calculation

Parameters	Convection coefficient W/(m ² ·°C)	Specific heat capacity J/(kg·°C)	Thermal conductivity W/(m·°C)
Values	13.3	480	56
Parameters	Absorptivity	Density (kg/m ³)	Emissivity
Values	0.6	7850	0.8
Parameters	Coefficient A	Coefficient B	Coefficient C
Values	1326.54	0.404	0.181
Parameters	Ground radiation reflectance ρ_g	c_N	
Values	0.15	1.0	

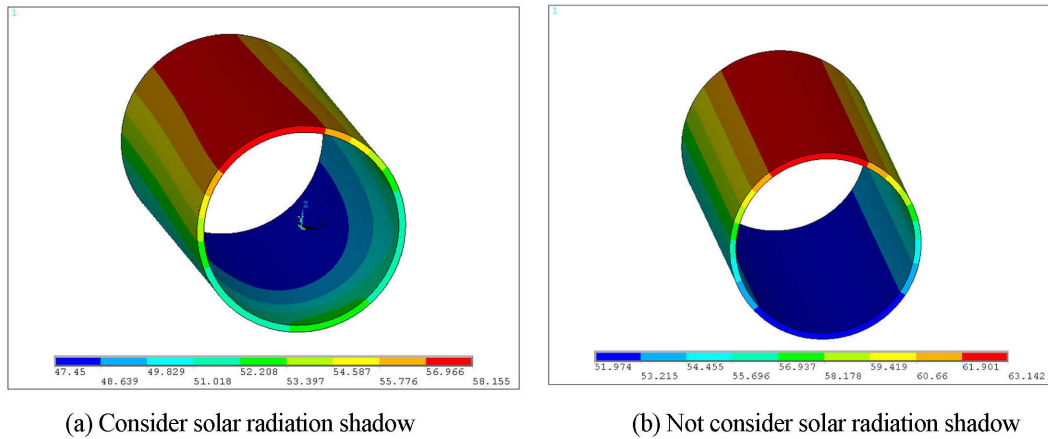


Fig. 8 Temperature field of steel tube specimen at 14:00 pm on 22th July 2010

4.4 Numerical analysis for the steel tube specimen

The temperature obtained from the transient analysis of each specimen is shown in Fig. 3~Fig. 4 and Table 1. It is clear that T_{FEL} (obtain from finite element analysis) is about 1.0-1.12 times higher than T_T (obtain from test data). It can be concluded that the strength T_{FEL} was generally consistent with the test results, with a maximum difference of 12.2%.

Reasons attributing to the discrepancies might include variance in the solar radiation model, variance in solar radiation absorption and ground reflectance, precision of infra-red temperature meter, etc. In the test process, the clouds may shelter against solar radiation, which induces the decrease of steel plate specimen's temperature. Taking these arguments into account, the FEM simulation results for the steel tube test specimen can be considered generally precise, and the transient FEM model can be used for future parametric studies.

The analyzed temperature distribution of the specimen at 14:00 on 22th July 2010 is shown in Fig. 8(a). It can be seen that the temperature field under solar radiation is very non-uniform. But the two ends of the steel tube are enclosed in practice. The temperature field of the steel tube specimen is analyzed under assumption that the solar radiation cannot irradiate the inner surface of specimen. The temperature field is shown in Fig. 8(b). From the FEM results, it can be concluded that the temperature along axis is uniform if the two ends of steel tubes is enclosed.

5. Parametrical studies

Parametric studies are conducted on the temperature distribution, in order to identify the dominant factors affecting the temperature distribution of steel tubes. The investigated parameters include the solar radiation absorption, the solar radiation reflectance of ground, angle β_s (as it shown in Fig. 9(a)), angle β_a (as it shown in Fig. 9(b)), angle β_e (as it shown in Fig. 9(c)), the thickness and the diameter of steel tube. The primary parameters of the FE model here is identical with the steel tube specimen. Transient thermal analysis is carried out for each model.

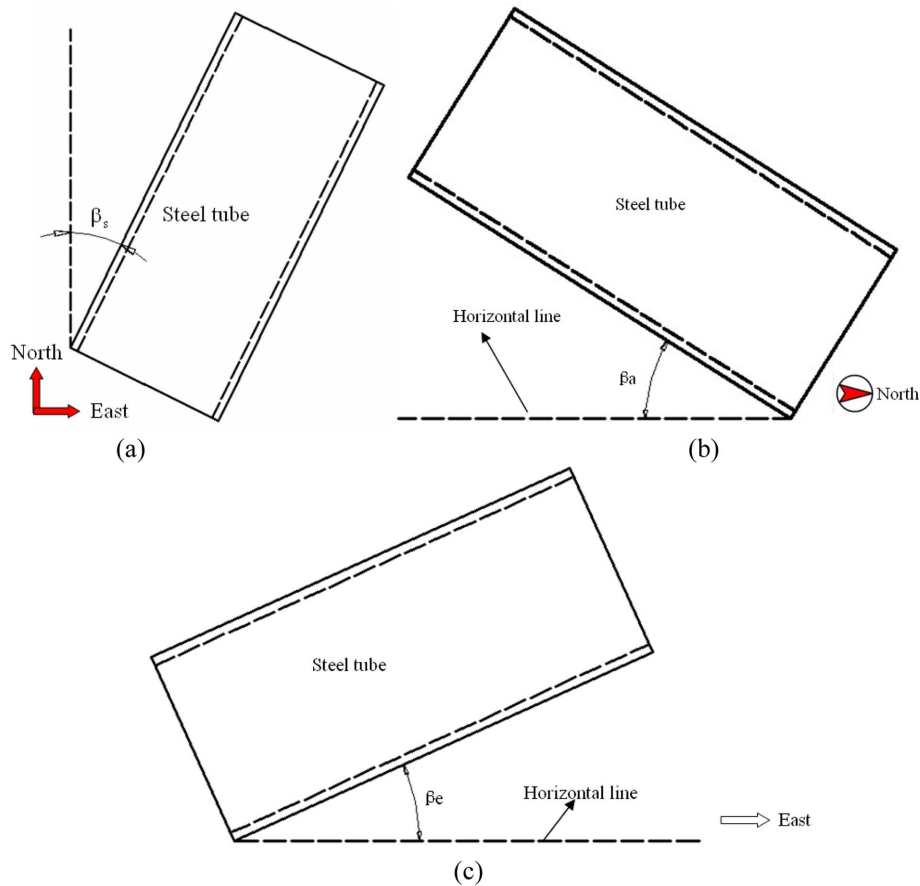


Fig. 9 Schematic diagram of angle β_s , β_a and β_e

Results from the parameter studies are shown in Fig. 10 to Fig. 16, from which it is clear that:

1) The solar radiation absorption has significant effect on the temperature distribution of steel tube. As indicated in Fig. 10, the temperature of steel tube under solar radiation increases with solar radiation absorption increases, and increment of the maximal temperature for each 0.1 of solar absorption is about 2.92°C ;

2) The ground solar radiation reflectance has little effect on the temperature distribution of steel tube under solar radiation. As indicated in Fig. 11, the temperature of steel tube under solar radiation increases with ground solar radiation reflectance, and increment of the maximal temperature for each 0.1 of solar absorption is about 0.56°C ;

3) The Angle β_s , Angle β_a and Angle β_e have significant effect on the temperature distribution of steel tube under solar radiation, shown as Figs. 12-14;

4) The thickness of steel tube has some effect on the temperature field under solar radiation. According to Fig. 15, the average decrease of the day maximal temperature for each 1 mm of steel tube thickness is about 0.69°C , and the average increment of the day minimal temperature for each 1mm of steel tube thickness is about 0.36°C .

5) The diameter of steel tube has significant effect on the temperature field under solar radiation.

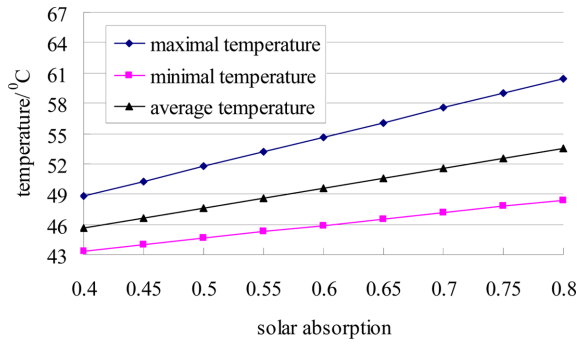


Fig. 10 Temperature under different radiation absorption at 14:00

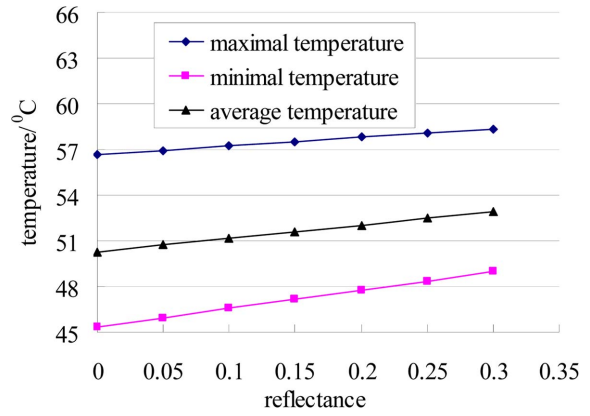


Fig. 11 Temperature under different radiation reflectance at 14:00

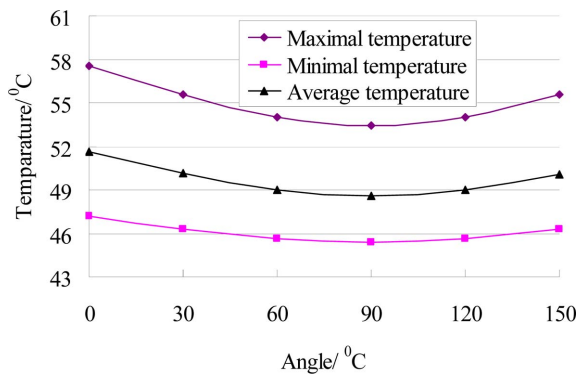


Fig. 12 Temperature under different angle β_s at 14:00

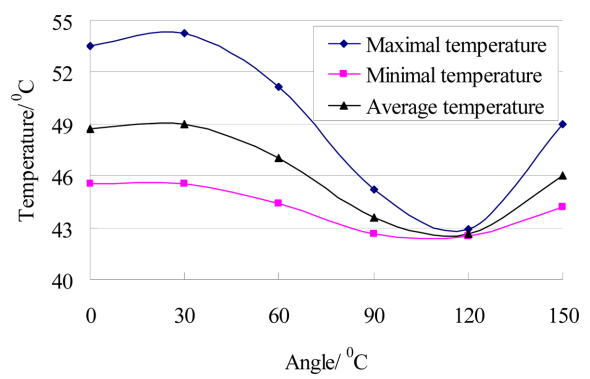


Fig. 13 Temperature under different angle β_a at 14:00

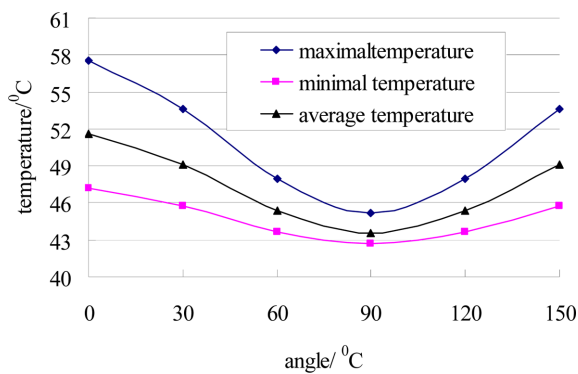


Fig. 14 Temperature under different angle β_e at 14:00

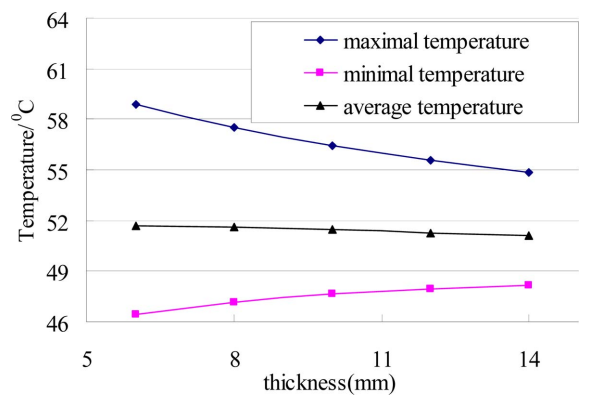


Fig. 15 Temperature under different thickness of tube at 14:00

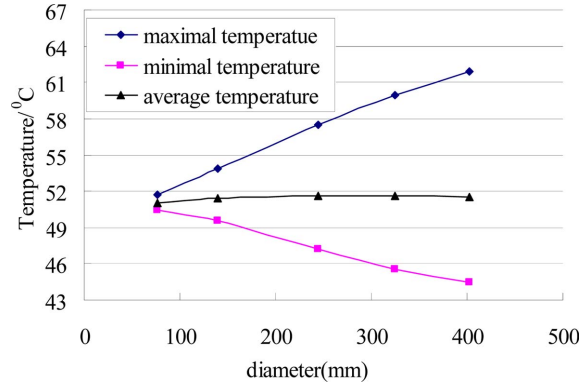


Fig. 16 Temperature under different diameter of tube at 14:00

From Fig. 16, the average increment of the day maximal temperature for each 100 mm of steel tube diameter is about 3.12°C, and the average decrease of the day minimal temperature for each 100 mm of steel tube diameter is about 1.69°C.

6. Simplified calculation method

6.1 calculation formulae

From the results of the experiment and the FEM analysis, it is clear that the temperature distribution along section direction is approximately following a sine curve and the temperature distribution along thickness direction is uniform. The temperature distribution of steel tubes along axis direction is uniform under solar radiation if the both ends are enclosed. Therefore, if the maximum temperature T_{\max} and minimal temperature T_{\min} along section of steel tube are obtained, the temperature distribution of steel tubes under solar radiation can be determined by following equation

$$T(\chi) = T_{\max} - (T_{\max} - T_{\min})\sin(\chi) \quad 0 < \chi \leq 360^\circ\text{C} \quad (8)$$

Where χ is the angle from the maximal temperature point in clockwise as shown in Fig. 7.

The maximal temperature point in the tube section is the point nearest to the sun, and the minimal temperature point is the farthest point to the sun. Considering that the change of the solar radiation and the air temperature is slow, the temperature of the nearest point and the farthest points from sun can be simply considered as steady-state temperature. The thermal flow acting on the surface around nearest point includes solar radiation, cross-convection and long wave radiation among sky, ground and steel tube surface. Therefore, the thermal balance equation can be determined as follows

$$q_S + q_L - h[T_a - T_{\max}] = 0 \quad (9)$$

Therefore

$$T_{\max} = \frac{(q_S + q_L)}{h} + T_a \quad (10)$$

In the Eq. (10), the parameter q_L is a fourth degree polynomial with corresponding steel temperature T so that it is very difficult to determine the steel temperature T through solving the Eq. (10). Therefore, temperature compensation method is recommended, and the steps for this method are as follows:

Step 1: Calculate the solar radiation q_S using Eq. (2) or Eq. (5).

Step 2: Give steel tube temperature T_{max} an estimated value t ; generally, the ambient air temperature T_a is set to estimated value t , that is $t = T_a$;

Step 3: Calculate the long wave radiation using Eq. (7);

Step 4: Calculate the steel temperature T_{max} using Eq. (10) based on the results of Step 1~Step 3.

Step 5: calculate the error between estimated value t and calculated value T_{max} using Eq. (11); if $error \leq error_{max}$, the steel tube temperature is T_{max} , otherwise, modify the estimated value t using Eq. (12), and recalculate the steel tube temperature from step 3~step 5

$$error = |T_{max} - t| \tag{11}$$

$$t = (T_{max} + t)/2 \tag{12}$$

For the farthest point, the thermal flow acting on the surface includes solar radiation, cross-convection, heat conduction and long wave radiation among sky, ground and steel tube surface. The thermal balance equation can be determined as following equation

$$\alpha \frac{4d^2(T_{max} - T_{min})}{\pi D} + q_S + q_L - h[T_a - T_{max}] = 0 \tag{13}$$

Therefore

$$T_{min} = \frac{\left(q_S + q_L + \alpha \frac{4d^2(T_{max} - T_{min})}{\pi D} \right)}{h} + T_a \tag{14}$$

6.2 Numerical example

The simplified calculation method is validated against the finite element transient thermal analysis. Fig. 17 shows the temperature distribution of steel tube specimen at 12 am on 22th July

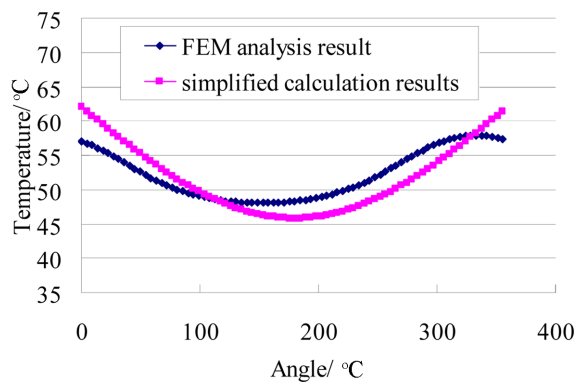


Fig. 17 Temperature calculated by simplified method

2010. It is clear that the calculated results agree well with that from transient FE thermal analysis. The simplified calculated method can be adopted to predict the temperature distribution of steel tube under solar radiation.

7. Conclusions

1) The daily temperature of the steel tube specimen was measured on 22th~24th July, 2010. From the test result, following conclusions are obtained: a) the temperature-time curve is similar to sine curve; b) maximal temperature obtained in this experiment is 54.3°C, which is 20.1°C higher than the corresponding ambient air temperature; c) the maximal temperatures usually occur at 11:00~14:00; d) the temperature field is very non-uniform under solar radiation.

2) Numerical simulation method presented in this paper can effectively predict the temperature distribution of steel tubes under solar radiation.

3) The temperature distribution of steel tubes under solar radiation is sensitive to the steel solar radiation absorption, steel tube diameter and orientation; but insensitive to the solar radiation reflectance and thickness of steel tube.

4) The simplified calculation method based on steady thermal finite element analysis can effectively predict the temperature distribution of steel tubes under solar radiation.

Acknowledgements

This work was supported by the National Natural Science Foundation of China (No.51208355), China Postdoctoral Science Foundation Funded Project (No.2012M510751) and Independent Innovation Funded Project of Tianjin University (No.1102).

References

- Alinia, M.M. and Kashizadeh, S. (2006), "Effect of flexibility of substructures upon thermal behaviour of spherical double layer space truss domes. Part I: Uniform thermal loading", *J. Constr. Steel Res.*, **62**(4), 359-368.
- Alinia, M.M. and Kashizadeh, S. (2006), "Effect of flexibility of substructures upon thermal behaviour of spherical double layer space truss domes. Part II: Gradient & partial loading", *J. Constr. Steel Res.*, **62**(7), 675-681.
- Alinia, M.M. and Kashizadeh, S. (2007), "Effects of support positioning on the thermal behaviour of double layer space truss domes", *J. Constr. Steel Res.*, **63**(3), 375-382.
- Chen, Z.H., Liu, H.B. and Zhou, T. (2009), *Parametric Analysis of Spatial Steel Structures Using APDL Language*, China WaterPower Press, Beijing. (in Chinese)
- Diefenderfer, B.K., Al-Qadi, I.L. and Diefenderfer, S.D. (2006), "Model to predict pavement temperature profile: development and validation", *J. Transp. Eng.-ASCE*, **132**(2), 162-167.
- Fan, Z., Wang, Z. and Tian, J. (2007), "Analysis on temperature field and determination of temperature upon heating of large-span steel structure of the National Stadium", *J. Buil. Struct.*, **28**(2), 32-40. (in Chinese)
- Huang, Z.F., Tan, K.H. and England, G.L. (2010), "Plastification procedure of laterally-loaded steel bars under a rising temperature", *Struct. Eng. Mech.*, **35**(6), 699-715.
- Jin, F., Chen, Z., Wang, J. and Yang, J. (2010), "Practical procedure for predicting non-uniform temperature on

- the exposed face of arch dams”, *Appl. Therm. Eng.*, **30**(14), 2146-2156.
- Kim, S.H., Cho, K.I., Won, J.H. and Kim, J.H. (2009), “A study on thermal behavior of curved steel box girder bridges considering solar radiation”, *Arch. Civil Mech. Eng.*, **9**(3), 59-76.
- Li, J. and Song, A. (1998), “Compare of clear day solar radiation model of Beijing and ASHRAE”, *J. Capital Normal Univ.*, **19**(1), 35-38. (in Chinese)
- McQuiston, F.C., Parker, J.D. and Jeffrey, D. (2005), *Spitler. Heating, Ventilating, and Air Conditioning Analysis and Design*, John Wiley and Sons, UAS.
- Papadopoulos, P.G., Papadopoulou, A.K. and Papaioannou, K.K. (2008), “Simple nonlinear static analysis of steel portal frame with pitched roof exposed to fire”, *Struct. Eng. Mech.*, **29**(3), 37-53.
- Tong, M., Tham, L.G. and Au, F.T.K. (2000), “Numerical modelling for temperature distribution in steel bridges”, *Comput. Struct.*, **79**(6), 583-593.
- Tong, M., Tham, L.G. and Au, F.T.K. (2002), “Extreme thermal loading on steel bridges in tropical region”, *J. Bridge Eng.*, **7**(6), 357-366.
- Xu, Y.L., Chen, B., Ng, C.L., Wong, K.Y. and Chan, W.Y. (2010), “Monitoring temperature effect on a long suspension bridge”, *Struct. Control Hlth.*, **17**(6), 632-653.